Phase separation in $Cu_{46}Zr_{47-x}Al_7Gd_x$ metallic glasses

Norbert Mattern [a,*], Ulla Vainio [b], Jin Man Park [a,c], Jun Hee Han [a], Ahmed Shariq [d], Do Hyang Kim [c], Jürgen Eckert [a,e]

[a] IFW Dresden, Institute for Complex Materials, Helmholtzstr. 20, 01069 Dresden, Germany
[b] HASYLAB at DESY, Notkestr. 85, 22603 Hamburg, Germany
[c] Center for Non-Crystalline Materials, Yonsei University, 134 Shinchon-dong, Seodaemun-ku, Seoul 120-749, South Korea
[d] FhG Center Nanoelectronic Technology, Koenigsbruecker Strasse 180, D-01099 Dresden, Germany
[e] TU Dresden, Institute of Materials Science, Helmholtzstr. 7, 01069 Dresden, Germany

ABSTRACT

The influence of Gd addition on phase separation of rapidly quenched $Cu_{46}Zr_{47-x}Al_7Gd_x$ metallic glasses ($x = 2,5,7$) was studied. For low Gd content ($x = 2$), a homogeneous glass is obtained for the as-quenched state. Annealing leads to cluster formation by nucleation and growth prior to crystallization. For the Gd contents $x = 5$ and 7, early stages of spinodal decomposition are observed in the as-quenched glasses. Further annealing increases the amplitude of the compositional fluctuations prior to crystallization. Atom probe tomography gives evidence of the presence of Gd-enriched clusters of 2–5 nm size for the $Cu_{46}Zr_{42}Al_7Gd_5$ glass. The structure formation as a function of the Gd content is essentially determined by the composition dependence of the miscibility gap of the metastable undercooled melt. Early stages of spinodal decomposition or almost homogeneous glassy states are obtained if the critical temperature of liquid–liquid phase separation is close or below to the glass transition temperature.

© 2010 Elsevier B.V. All rights reserved.

1. Introduction

Bulk metallic glasses (BMGs) have been developed in a number of different alloy systems, such as Cu-, Zr-, Mg-, and Fe-based alloys [1]. Among them, Cu-based BMGs have been shown to be excellent candidates for structural applications due to their high strength, high glass-forming ability (GFA), high thermal stability and inexpensiveness [2,3]. For the BMG-forming alloys, the number of components, the atomic size of the constituent elements, the composition and the cohesion between the metals are some of the crucial factors for the glass formation. Therefore, minor addition of an element plays an effective role for the glass-forming ability (GFA) and the properties of the BMGs [4]. Recently, it was found that the addition of gadolinium dramatically increased the GFA of Cu-based alloys, and BMGs with a diameter of 10 mm could be obtained for $Cu_{46}Zr_{45}Al_7Gd_2$ [5]. The occurrence of phase separation was recently reported for rapidly quenched glassy $Cu_{46}Zr_{47-x}Al_7Gd_x$ alloys with Gd contents $15 < x < 40$ [6]. For low concentration of gadolinium ($x = 2$), an enhanced plasticity is obtained which has been explained as being related to local chemical heterogeneity in the amorphous matrix however without any direct evidence for that.

In this paper, we report on the influence of the gadolinium content on the formation and transformation of the early stages of phase separation in $Cu_{46}Zr_{47-x}Al_7Gd_x$ glasses. In situ small-angle X-ray scattering (SAXS) at elevated temperatures was applied in combination with simultaneous X-ray diffraction (XRD) in order to analyse the temperature and time dependence of the decomposition, and especially to clarify whether phase separation occurs prior to crystallization.

2. Experimental

Pre-alloyed ingots were prepared by arc-melting elemental Cu, Zr, Gd and Al with purities of 99.9% or higher in a Ti-gettered argon atmosphere. To ensure homogeneity, the samples were remelted several times. From these pre-alloys, thin ribbons (3 mm in width and 30 μm in thickness) with nominal compositions $Cu_{46}Zr_{47-x}Al_7Gd_x$ $x = 2,5,7$ were prepared by single-roller melt spinning under argon atmosphere. Differential scanning calorimetry (DSC) experiments were performed employing a Netzsch DSC 404 calorimeter with a heating rate of 20 K/min. Small angle X-ray scattering (SAXS) was measured at the B1 synchrotron beam line of HASYLAB/DESY using an energy of 16516 eV. Samples were mounted on a heating stage which was used under vacuum for in situ measurements. Intensity curves were registered by a PILATUS 300k area detector at a distance covering a q-range between 0.2 and 4.3 nm^{-1}. SAXS provides integral information on existing inhomogeneities in electron density with a size ranging from the nanometre up to the micron range [7]. Simultaneously wide angle X-ray scattering (WAXS) patterns were recorded by a linear position sensitive detector (MYTHEN). The sample temperature was stepwise ($\Delta T = 10$ K) increased from $T = 573$–873 K after 30 min of each measurement. A dual focus ion beam system (FEI Strata 400) was used for the fabrication of the atom probe tomography (APT) tips. The specimens were then analysed using the local electrode atom probe (LEAP 3000 X Si^{TM}) equipped with diode-pumped solid-state
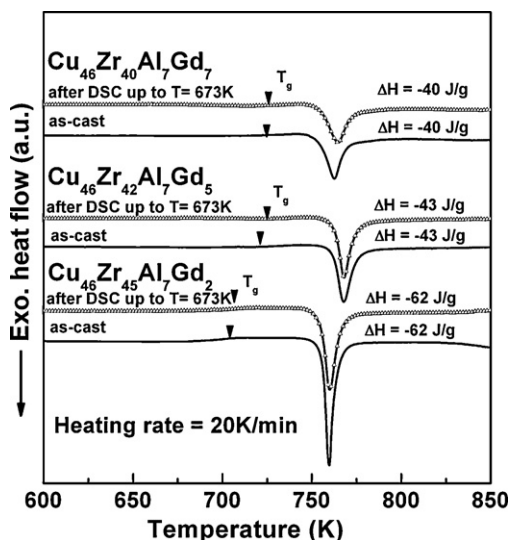
Fig. 1. DSC scans of as-quenched glassy $Cu_{46}Zr_{47-x}Al_7Gd_x$ alloys (x = 2,5,7), and after heat treatment (DSC heating up to 673 K and cooling down to room temperature with 20 K/min).

laser operating at the second harmonic frequency of 532 nm with a pulse duration of ~10 ps and a laser spot size <10 μm. Pulse laser atom probe analyses were carried out at 27 K and an average detection rate of 0.005 ions/pulse.

3. Results

Fig. 1 shows the thermal behaviour of the $Cu_{46}Zr_{47-x}Al_7Gd_x$ glasses by their DSC traces. The occurrence of the glass transition in a range of about $T_g \approx 700$ K and the exothermic crystallization event at about $T_x \approx 750$ K are clear evidence for the glassy nature of the samples in the as-quenched state which is preserved after annealing the ribbons by DSC-heating up to T = 673 K. The TEM image shown in Fig. 2 and the XRD patterns of the as-quenched state depicted in Figs. 3–5 confirm the almost complete amorphous structure of the as-quenched state. Some fluctuations can be seen in the contrast of the TEM image, which are probably caused by preparation, as also observed for other Cu–Zr based metallic glasses [8].
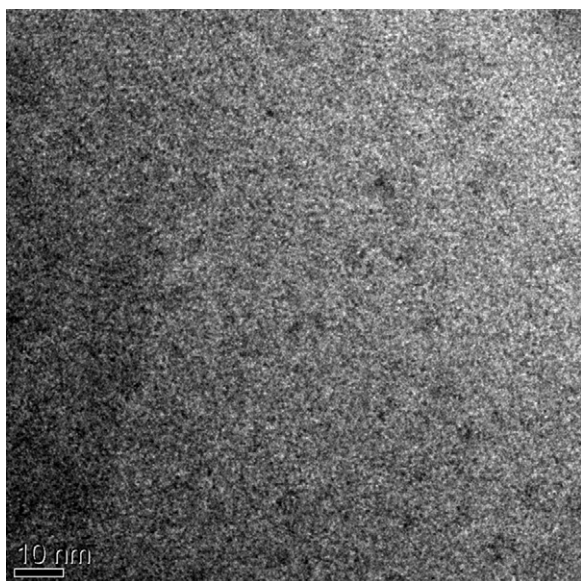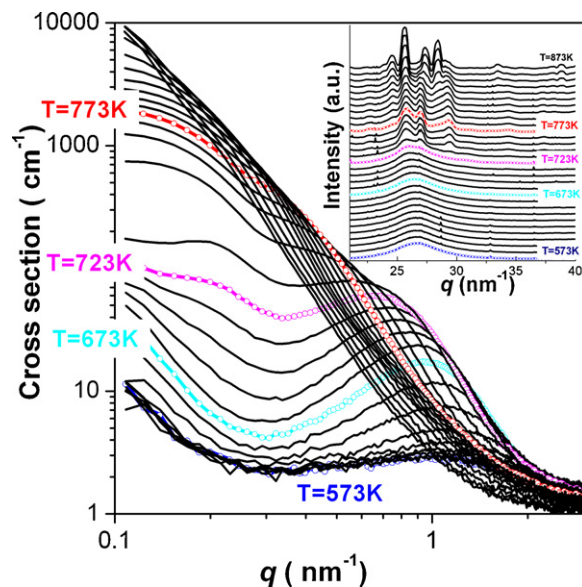

Fig. 2. TEM image of $Cu_{46}Zr_{42}Al_7 Gd_5$ metallic glass.
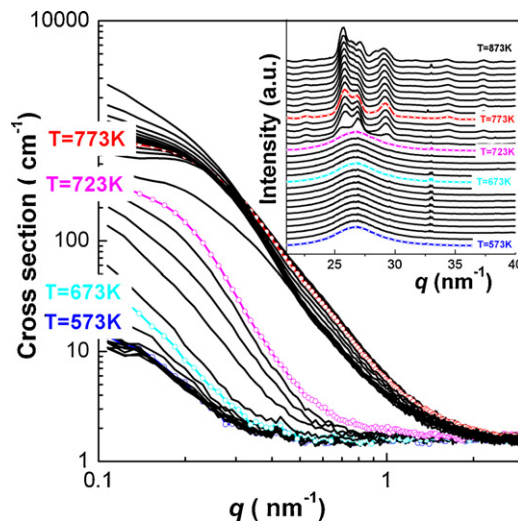
Fig. 3. In situ SAXS and WAXS (inset) at different temperatures for glassy $Cu_{46}Zr_{45}Al_7Gd_2$.

Fig. 3 shows the SAXS curves for the $Cu_{46}Zr_{45}Al_7Gd_2$ metallic glass. The simultaneously measured WAXS patterns are also given in the inset. A very low SAXS intensity is observed for the as-quenched state which remains unchanged till a temperature of T = 573 K which shown as distinguished curve. Therefore, the as-quenched state of the $Cu_{46}Zr_{45}Al_7Gd_2$ ribbons is homogeneous without any indication of phase separation. Upon heating at temperatures between T = 663 K and 713 K the SAXS intensities increase gradually. This behaviour indicates nucleation and growth of heterogeneities in the glass well below the crystallization temperature T_x. The change of the intensity of the SAXS curves for temperatures between T = 653 and 723 K points to formation of uncorrelated, randomly distributed clusters with a certain size distribution. Up to T = 713 K the WAXS patterns remain unchanged, which means that the glassy structure is retained. This is also confirmed by the DSC scan of the sample preheated up to T = 673 K before, as given in Fig. 1, which clearly shows unchanged glass transition and crystallization enthalpy compared to the as-quenched state. The onset of

Fig. 4. In situ SAXS and WAXS (inset) at different temperatures for glassy $Cu_{46}Zr_{42}Al_7Gd_5$.

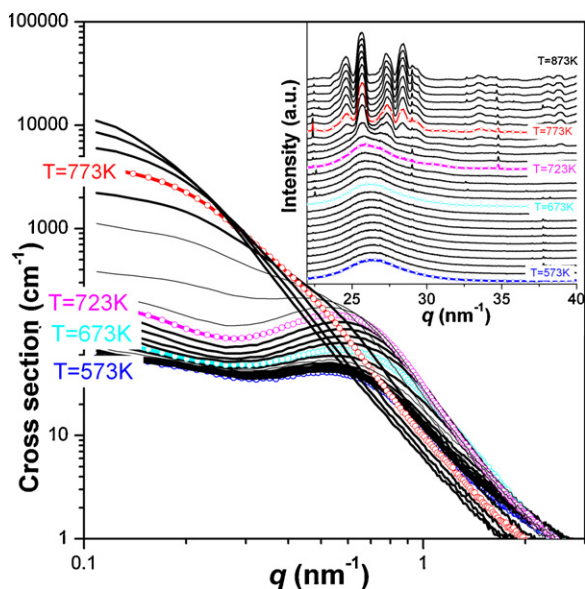**Fig. 5.** In situ SAXS and WAXS (inset) at different temperatures for glassy $Cu_{46}Zr_{40}Al_7Gd_7$.

crystallization at $T = 733$ K is reflected by an abrupt change of the shape and the intensity of the SAXS versus temperature.

The SAXS and WAXS patterns of the $Cu_{46}Zr_{42}Al_7Gd_5$ metallic glass shown in Fig. 4 behave completely different for the alloy with higher gadolinium content. A weak correlation maximum at $q_{max} = 1.2$ nm^{-1} is observed in the SAXS curve of the as-quenched state identical with the given distinguished curve at $T = 573$ K. The interference maximum indicates the presence of compositional fluctuations with a dominant correlation length. Using the relationship $\zeta = 2\pi/q_{max}$ between the correlation length ζ and the position of the maximum q_{max} one obtains a value of $\zeta = 5$ nm. Upon heating from $T = 603$–673 K the intensity of the maximum increases obviously but the position q_{max} becomes only slightly shifted. Such behaviour is typical for early stages of spinodal decomposition where first the amplitudes of the chemical fluctuations increase [9]. DSC scan of the sample preheated up to $T = 673$ K confirms the preservation of the glassy structure (Fig. 1). With further increasing temperature up to $T = 713$ K we observe an on-going phase separation prior to crystallization, which starts at $T_x = 723$ K for the step-wise heating. Again, with the onset of the crystallization at $T = 723$ K an abrupt change of the shape and the intensity of the SAXS occurs.

Fig. 5 shows the SAXS curves for the $Cu_{46}Zr_{40}Al_7Gd_7$ metallic glass. A distinct correlation maximum at $q_{max} = 0.7$ nm^{-1} is observed in the SAXS curve of the as-quenched state which is identical with the distinguished curve at $T = 573$ K. This indicates ongoing phase separation by a spinodal mechanism already during quenching with a dominant correlation length of about 9 nm. Upon heating up to 723 K the maximum increases in intensity at an almost unchanged position of q_{max}. The preservation of the glassy structure is expressed by the diffuse character of the corresponding WAXS pattern as well as by the DSC scan for a ribbon annealed at $T = 673$ K (Fig. 1). With the onset of the crystallization at $T_x = 733$ K an abrupt change of the shape and the intensity of the SAXS occurs.

The occurrence of phase separation in the $Cu_{46}Zr_{42}Al_7Gd_5$ metallic glass is also confirmed by APT investigations. Fig. 6 shows for the as-cast state the spatial distribution of the constituent elements and iso-concentration surfaces for 10 at% Gd are drawn to elaborate the interface regions of the Gd-enriched clusters. The counted numbers of atoms by the APT data give the chemical composition $Cu_{46.1}Zr_{41.6}Al_{7.5}Gd_{4.8}$, which is in a good agreement with
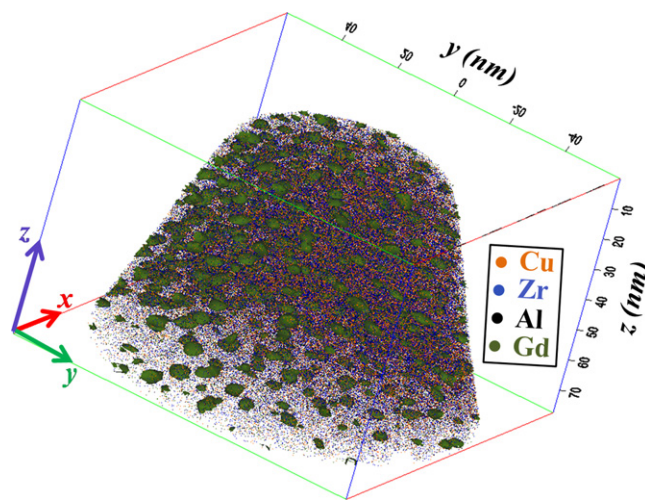

Fig. 6. Spatial distribution of the constituent elements of as-quenched glassy $Cu_{46}Zr_{42}Al_7Gd_5$ as analysed by atom probe tomography. Iso-concentration surface (10 at%Gd) is drawn in green to elaborate the Gd-enriched clusters (for clarity, not 100% of the atoms Cu [orange], Zr [blue], Al [black] are shown).

the nominal value. The 3D-AP micrograph clearly shows a heterogeneous structure with Gd-enriched clusters distributed throughout the analysed volume having diameter in a range 2–5 nm. The concentration profile from a cylinder 3 nm in diameter through the volume is given in Fig. 7. The Gd-enriched clusters contain a relatively higher amount of Cu, however are depleted in Zr and Al. The chemical composition of clusters with the highest Gd-content is about $Cu_{65}Zr_{15}Gd_{20}$.

4. Discussion

Fig. 8 shows a section of the calculated Cu–Gd–Zr phase diagram using the CALPHAD method. The assessment was done by an extrapolation of the corresponding three binary phase diagrams [10–12]. The calculation can be treated only as a first approximation because ternary interactions are unknown and the contribution of Al is neglected. However, qualitatively the calculations should describe the phase relations correctly for the composition range of the samples having only a low Al content. A metastable miscibility gap of the undercooled melt follows from the thermodynamic assessment, as indicated by the bimodal curve. The CALPHAD calculation for $Cu_{50}Zr_{45}Gd_5$ at $T = 500$ K results in the existence of

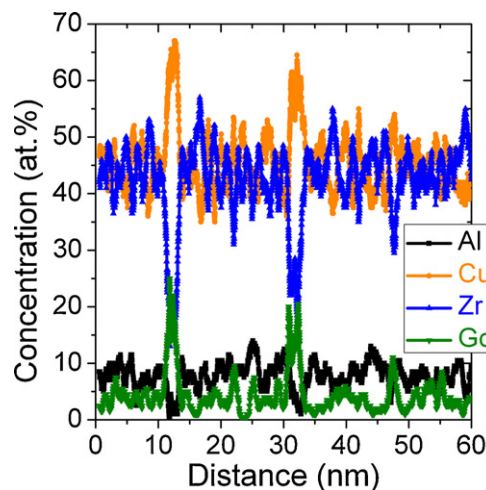**Fig. 7.** Compositional depth profile of glassy $Cu_{46}Zr_{42}Al_7Gd_5$ from a selected cylinder of 3 nm diameter.

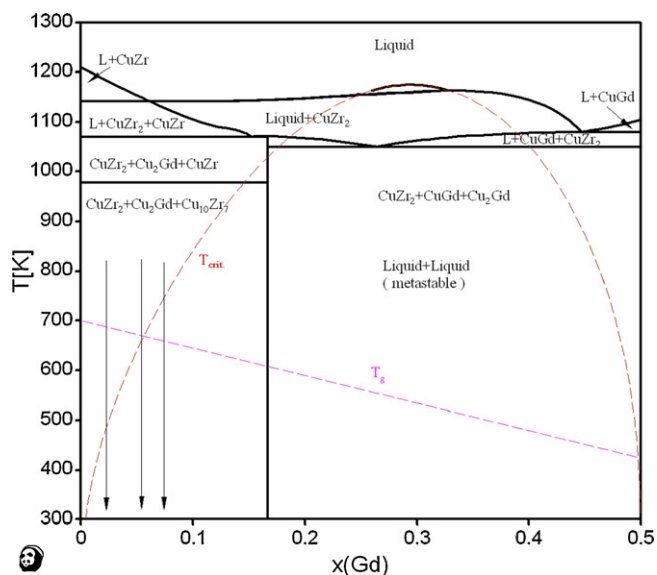**Fig. 8.** Pseudo-binary section $Cu_{50}Zr_{50}$–$Cu_{50}Gd_{50}$ of the ternary Cu–Zr–Gd phase diagram.

two liquids for the metastable equilibrium with the compositions $Cu_{49}Zr_{49}Gd_2$ (92 vol%), and $Cu_{62}Zr_2Gd_{36}$ (8 vol%). The calculated values describe the trend of the experimental observation of the phase separation in the rapidly quenched $Cu_{50}Zr_{45}Gd_5$ glass. The critical temperature of liquid–liquid phase separation $T_{crit.}$ is rather low for a Gd-content $x = 2$–7, and is only slightly different from the glass transition temperature T_g. From this picture it is understandable that early stages of spinodal decomposition ($x = 5,7$) or even an almost homogeneous ($x = 2$) glass can be frozen in if crystallization is avoided during rapid quenching. Annealing the glass afterwards at elevated temperatures below the crystallization temperature leads to phase separation by nucleation and growth ($x = 2$) or fur-

ther development of already frozen-in fluctuations by a spinodal mechanism ($x = 5,7$).

5. Conclusions

Phase separated metallic glasses can be prepared in the Cu–Zr–Al–Gd system by rapid quenching of the melt. The formed microstructure is essentially determined by the critical temperature of liquid–liquid phase separation, which is a function of the chemical composition of the alloy. An almost homogeneous glassy state or early stages of spinodal decomposition are obtained if T_{crit} is close to the glass transition temperature T_g. Evidence of ongoing phase separation prior to crystallization could be observed by in situ measurements at elevated temperature. For low Gd-content ($x \leq 2$) complete solubility of Gd in the CuZr glass occurs as a consequence of the thermodynamic properties of the undercooled melt.

References

[1] M. Miller, P. Liaw (Eds.), Bulk Metallic Glasses, Springer, 2008.
[2] X.H. Lin, W.L. Johnson, J. Appl. Phys. 78 (1995) 6514.
[3] A. Inoue, W. Zhang, T. Zhang, K. Kurosaka, Acta Mater. 49 (2001) 2645.
[4] W. Zhang, A. Inoue, Mater. Trans. 45 (2004) 532.
[5] H.M. Fu, H. Wang, H.F. Zhang, Z.Q. Hu, Scripta Mater. 55 (2006) 147.
[6] E.S. Park, J.S. Kyeong, D.H. Kim, Scripta Mater. 57 (2007) 49.
[7] O. Glatter, O. Kratky, Small-Angle X-Ray Scattering, Academic Press, London, 1982.
[8] G. Kumar, T. Ohkubo, T. Mukai, K. Hono, Scripta Mater. 57 (2007) 173.
[9] K. Binder, P. Fratzl, in: G. Kostorz (Ed.), Phase Transformations in Material, Wiley/VCH, Weinheim, 2001, p. 409.
[10] K.J. Zen, M. Hamalainen, H.L. Lukas, J. Phase Equilib. 15 (1994) 577.
[11] A.L. Voskov, I.A. Uspenskaya, Russ. J. Phys. Chem. A 83 (2009) 604.
[12] M. Zinkevich, N. Mattern, H.J. Seifert, J. Phase Equilib. 22 (2001) 43.